00360, and receipt of an NIH Research Career Development Award (CA-00015).

Appendix

The calculations were performed using the extended Hückel method.[25] The H_{ii}'s and orbital exponents for Fe were taken from previous work.[17] The hydrogen H_{il} was set at -10.0 eV. This places the hydrogens energywise above the valence orbitals of the cluster, giving the H's the character of protons. Calculations with hydrogen H_{ii}'s at -13.6 eV, our normal value, result in a slight change in the magnitude of the calculated energy differences, but do not alter the conclusions reached. The parameters are given in Table III.

The metal-metal distance was kept at 2.54 Å and the cluster geometry tetrahedral. The Fe-C distance in the carbonyl cluster was 1.8 Å, and the distance from the metal to the center of the cyclopentadiene ring in Fe_4Cp_4 was 1.7 Å. The hydrogens were placed 0.86 Å above the cluster face and 1.14 Å from the edge in the face- and edge-protonated systems, respectively.

References and Notes

(1) (a) Cornell University; (b) University of Southern California; (c) University of California; (d) University of Oxford.
(2) (a) R. Saillant, G. Barcelo, and H. D. Kaesz, *J. Am. Chem. Soc.*, **92**, 5739 (1970); (b) R. D. Wilson and R. Bau, *ibid.*, **98**, 4687 (1976).
(3) H. D. Kaesz, B. Fontal, R. Bau, S. W. Kirtley, and M. R. Churchill, *J. Am. Chem. Soc.*, **91**, 1021 (1969).
(4) (a) H. D. Kaesz, S. A. R. Knox, J. W. Koepke, and R. B. Saillant, *Chem. Commun.*, 477 (1971); S. A. R. Knox and H. D. Kaesz, *J. Am. Chem. Soc.*, **93**, 4594 (1971); (b) B. F. G. Johnson, R. D. Johnston, J. Lewis, B. H. Robinson, and G. Wilkinson, *J. Chem. Soc. A*, 2856 (1968).
(5) R. D. Wilson, S. M. Wu, R. A. Love, and R. Bau, *Inorg. Chem.*, **17**, 1271 (1978).
(6) J. R. Shapley, S. I. Richter, M. R. Churchill, and R. A. Lashewycz, *J. Am. Chem. Soc.*, **99**, 7384 (1977).
(7) J. Müller and H. Dorner, *Angew. Chem.*, **85**, 867 (1973); *Angew. Chem., Int. Ed. Engl.*, **12**, 843 (1973).
(8) G. Huttner and H. Lorenz, *Chem. Ber.*, **108**, 973 (1975).
(9) J. Müller, H. Dorner, G. Huttner, and H. Lorenz, *Angew. Chem.*, **85**, 1117 (1973); *Angew. Chem., Int. Ed. Engl.*, **12**, 1005 (1973).
(10) G. Huttner and H. Lorenz, *Chem. Ber.*, **107**, 996 (1974).
(11) T. F. Koetzle, R. K. McMullan, R. Bau, D. W. Hart, R. G. Teller, D. L. Tipton, and R. D. Wilson, *Adv. Chem. Ser.*, in press.
(12) K. Wade, *Chem. Commun.*, 792 (1971); *Inorg. Nucl. Chem. Lett.*, **8**, 559, 563 (1972); "Electron Deficient Compounds", Nelson, London, 1971; *Adv. Inorg. Chem. Radiochem.*, **18**, 1 (1976).
(13) D. M. P. Mingos, *Nature (London), Phys. Sci.*, **236**, 99 (1972); R. Mason and D. M. P. Mingos, *MTP Int. Rev. Sci.: Phys. Sci., Ser. Two*, **11**, 121 (1975); D. M. P. Mingos and M. I. Forsyth, *J. Chem. Soc., Dalton Trans.*, 610 (1977).
(14) Trinh-Toan, W. P. Fehlhammer, and L. F. Dahl, *J. Am. Chem. Soc.*, **94**, 3389 (1972); A. S. Foust, M. S. Foster, and L. F. Dahl, *ibid.*, **91**, 5633 (1969).
(15) J. W. Lauher, to be published.
(16) M. Elian, M. M.-L. Chen, D. M. P. Mingos, and R. Hoffmann, *Inorg. Chem.*, **15**, 1148 (1976). See also ref 12–15 and J. E. Ellis, *J. Chem. Educ.*, **53**, 2 (1976).
(17) T. A. Albright, P. Hofmann, and R. Hoffmann, *J. Am. Chem. Soc.*, **99**, 7546 (1977).
(18) M. Elian and R. Hoffmann, *Inorg. Chem.*, **14**, 1058 (1975).
(19) See R. Hoffmann and W. N. Lipscomb, *J. Chem. Phys.*, **36**, 2179 (1962), for a discussion of this problem in the boron hydrides.
(20) C. Glidewell, *Inorg. Nucl. Chem. Lett.*, **11**, 761 (1975).
(21) R. B. King, *Inorg. Chem.*, **16**, 1822 (1977); R. B. King and D. H. Rouvray, *J. Am. Chem. Soc.*, **99**, 7834 (1977).
(22) S. F. A. Kettle, *Theor. Chim. Acta*, **4**, 150 (1966); S. F. A. Kettle and V. Tomlinson, *ibid.*, **14**, 175 (1969); *J. Chem. Soc. A*, 2002, 2007 (1969); S. F. A. Kettle and D. J. Reynolds, *Theor. Chim. Acta*, **22**, 239 (1971).
(23) M. A. Andrews and H. D. Kaesz, to be published.
(24) J. W. Koepke, J. R. Johnson, S. A. R. Knox, and H. D. Kaesz, *J. Am. Chem. Soc.*, **97**, 3947 (1975).
(25) R. Hoffmann, *J. Chem. Phys.*, **39**, 1397 (1963); R. Hoffmann and W. N. Lipscomb, *ibid.*, **36**, 2179, 3489 (1962); **37**, 2872 (1962).

The Band Structure of the Tetracyanoplatinate Chain

Myung-Hwan Whangbo and Roald Hoffmann*

Contribution from the Department of Chemistry, Cornell University, Ithaca, New York 14853. *Received September 6, 1977*

Abstract: The band structure of the tetracyanoplatinate chain is examined in the tight-binding approximation based on the extended Hückel method. The unit cell contains a staggered $[Pt(CN)_4]_2^{4-}$, and the calculation is repeated at various Pt-Pt separations. The free electron nature of the bands is probed by computing effective masses. From the band structure and the density of states one derives an expression for the total energy per unit cell as a function of partial oxidation of the polymer. The equilibrium Pt-Pt separation so estimated decreases to less than 3 Å for a loss of 0.3 electron per platinum, in reasonable agreement with structural studies. Details of the band structure are supported by explicit and simple molecular orbital arguments.

A class of partially oxidized one-dimensional conducting salts of tetracyanoplatinate, $Pt(CN)_4^{2-}$, has been one of the most extensively studied low-dimensional conducting materials.[1] The crystal structures of these compounds contain the planar platinum complex, $Pt(CN)_4^{2-}$, stacked together to form parallel linear or nearly linear chains of Pt atoms.[2] Structural and chemical observations on these compounds reveal that the Pt atoms are all equivalent, and thus they are in a single partial oxidation state, and that the Pt-Pt distance (r_{Pt-Pt}) becomes shorter with increase in the partial oxidation number of Pt.[2] In a band picture the fractional oxidation state of Pt corresponds to a partially filled band. Experiments on $K_2[Pt(CN)_4]Br_{0.3}\cdot 3H_2O$ (KCP) indicate that except for the Peierls instability the conduction electrons in KCP behave as nearly free electrons along the Pt chain.[3] Further, this free electron character persists among the analogues of KCP despite a large variation of r_{Pt-Pt} in these compounds.

Calculations of the band structure of the $Pt(CN)_4^{2-}$ chain reported so far have considered in general only a linear chain of Pt atoms.[4,5] A three-band model (i.e., inclusion of $5d_{z^2}$, 6s and $6p_z$ of Pt, where z refers to the Pt-chain axis) was found inadequate for the description of the electronic structure of KCP.[4a] Under the assumption that the CN^- ligands force the Pt atom to adopt a wave vector independent s-d hybridization, a two-band model (i.e., inclusion of s-d hybrid and p_z orbitals) produces a free-electron-like band.[4a] An important recent calculation by Bullett considers the full $Pt(CN)_4^{2-}$ chain.[5b]

In the present work the band structure of the $Pt(CN)_4^{2-}$ chain was examined within the tight-binding scheme[6] based upon the extended Hückel method.[7] Our calculations included all the valence atomic orbitals of the Pt, C, and N atoms of a unit cell in the $Pt(CN)_4^{2-}$ chain. Questions of theoretical importance in the electronic structure of the $Pt(CN)_4^{2-}$ chain are (a) the free-electron behavior of the conduction electrons

0002-7863/78/1500-6093$01.00/0

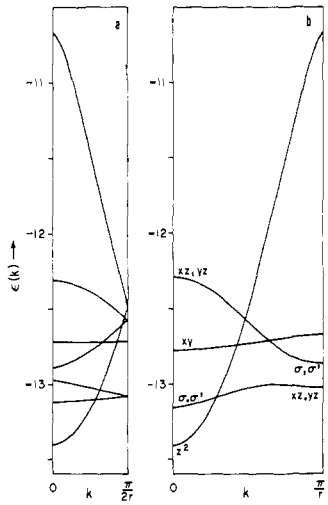

Figure 1. The occupied d-block bands of the $Pt(CN)_4^{2-}$ chain. Alternate $Pt(CN)_4^{2-}$ units are (a, left) staggered and (b, right) eclipsed. In all the figures energies are in eV.

in the partially filled band and its apparent independence of r_{Pt-Pt} and (b) the shortening of r_{Pt-Pt} with the increasing oxidation of Pt, or equivalently with greater electron removal from the partially filled band. In the following these problems were examined in some detail by considering the density of states for the partially filled band and the total energy per unit cell as a function of r_{Pt-Pt}, in addition to band structure calculations.

Our previous experience with approximate molecular orbital calculations for organic and inorganic molecules has taught us that it is useful to strive for a detailed understanding of the way that energy levels behave with respect to some geometrical or electronic perturbation based on simple ideas of symmetry, overlap, and bonding. The resulting qualitative arguments are a check on the calculations and allow extrapolation to other systems based on chemical intuition. In this, the first of a series of papers on the electronic structure of real and potential conducting systems, we intend to take some space to explain to a chemical audience why the computed bands come out the way that they do.[8] While in the process we run the risk of saying things that are obvious to solid-state theorists or to chemists knowledgeable in the area, we are willing to take that risk in view of the great potential benefit of building true bridges of comprehension between chemistry and physics.

Theoretical Procedure

The tight-binding method[6] of band structure calculation and the band structures[9] of many one-dimensional systems obtained by the extended Hückel method are well documented in the literature. Given a set of basis atomic orbitals $\{\chi_\mu\}$ for the atoms of a unit cell, the set of the Bloch basis orbitals $\{b_\mu(\mathbf{k})\}$ are formed as

$$b_\mu(\mathbf{k}) = N^{-1/2} \sum_\ell e^{i\mathbf{k}\cdot\mathbf{R}_\ell} \chi_\mu(r - \mathbf{R}_\ell) \quad (1)$$

where $\mathbf{k}$ is the wave vector, and $\mathbf{R}_\ell = \ell\cdot\mathbf{a}$ with $\mathbf{a}$ being the primitive vector. With these Bloch basis orbitals the extended Hückel method leads to the eigenvalue equation.

$$H(\mathbf{k})C(\mathbf{k}) = S(\mathbf{k})C(\mathbf{k})e(\mathbf{k}) \quad (2)$$

where $H_{\mu\nu}(\mathbf{k}) = \langle b_\mu(\mathbf{k})|H_{\text{eff}}|b_\nu(\mathbf{k})\rangle$ and $S_{\mu\nu} = \langle b_\mu(\mathbf{k})|b_\nu(\mathbf{k})\rangle$. The solution of this eigenvalue problem results in LCAO-crystal orbitals $\psi_n(\mathbf{k})$

$$\psi_n(\mathbf{k}) = \sum_\mu C_{n\mu}(\mathbf{k})b_\mu(\mathbf{k}) \quad (3)$$

and eigenvalues $\epsilon_n(\mathbf{k})$. The band structure is then determined by performing the above calculation for various values of $\mathbf{k}$ (usually within the first Brillouin zone; $-0.5K \le \mathbf{k} \le 0.5K$, where $K = 2\pi/\mathbf{a}$). The parameters of the extended Hückel calculation are detailed in the Appendix.

Partially oxidized salts of the $Pt(CN)_4^{2-}$ chain show the staggered arrangement of alternate $Pt(CN)_4^{2-}$ units, **1**.

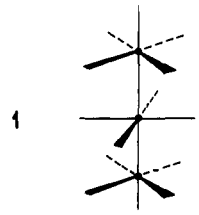

Therefore a unit cell contains two $Pt(CN)_4^{2-}$ units, and the primitive vector $\mathbf{a}$ becomes $2r_{Pt-Pt}$. In our calculations lattice sums were carried out to nearest neighbors (i.e., $\ell = -1, 0, 1$ in eq 1), and eq 2 was solved at $\mathbf{k} = 0.0, 0.1, 0.2, 0.3, 0.4$, and $0.5K$. These calculations were repeated by varying r_{Pt-Pt} from 2.5 to 3.8 Å, in which the Pt-C and C-N bond lengths were fixed at 2.06 and 1.19 Å, respectively. The coupling of the Pt-Pt separation with relative orientation of the monomer units will not be discussed in this paper.

Band Structure

A. The Occupied d-Block Band. Figure 1 shows the top portion of the occupied bands (i.e., the occupied d block) for $r_{Pt-Pt} = 2.88$ Å. Figures 1a and 1b refer to the cases when alternate $Pt(CN)_4^{2-}$ units in the chain are staggered and eclipsed, respectively. In the latter case, a unit cell contains only one $Pt(CN)_4^{2-}$ unit, and the lattice sums in the band calculation were carried out to second-nearest neighbors.

Figure 1 reveals that the d_{z^2} band, which becomes a conduction band upon partial oxidation, overlaps with other bands.[10] At various values of $\mathbf{k}$, the ratio of the coefficients of the 6s and $5d_{z^2}$ orbitals in the LCAO-crystal orbitals of the d_{z^2} band is almost constant (~0.26), which supports the assumption of a $\mathbf{k}$-independent s-d hybridization of Pt introduced in the two-band model.[4a] In Figure 1b the symbols σ and σ' indicate that the crystal orbitals are largely composed of the σ_{CN} orbitals as depicted below in **2** and **3**. These orbitals have

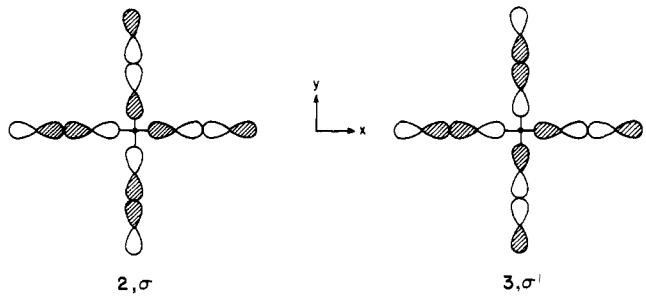

the proper symmetry to combine with the d_{xz} and d_{yz} orbitals of neighbor unit cells. The two degenerate bands (denoted by xz and yz and by σ and σ' at the zone center) interchange their character as one approaches the zone edge.

The essential features of the band structure of the staggered arrangement are almost the same as those of the eclipsed geometry. Simply speaking, the band structure of Figure 1a may be described as if the second half of the band structure of Figure 2b were folded back onto its first half. The slight discrepancy between Figure 1a and this folded structure comes from small differences in the overlap integrals between the basis orbitals of $Pt(CN)_4^{2-}$ units in the staggered and eclipsed arrangements. In Figure 1a all the bands are doubly degenerate except for the d_{z^2} band.

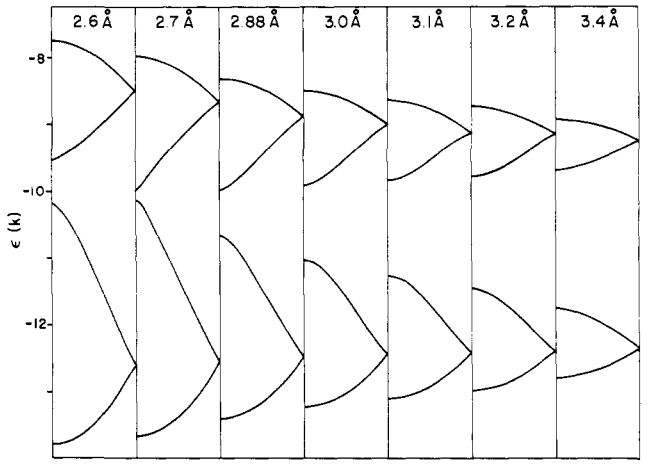

Figure 2. The band structure of the $Pt(CN)_4^{2-}$ chain as a function of r_{Pt-Pt}. Each column shows the d_{z^2} (lower part) and the p_z (upper part) bands in the region $0 \leq \mathbf{k} \leq K/2$.

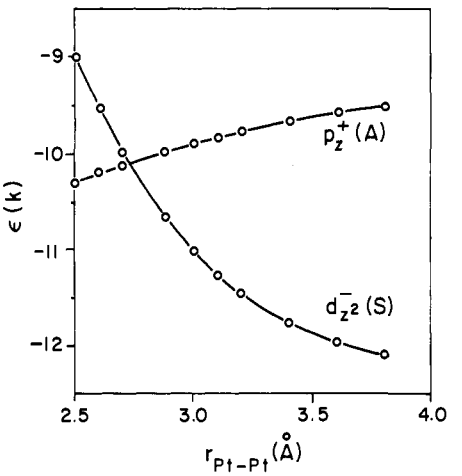

Figure 3. The top of the d_{z^2} band and the bottom of the p_z band as a function of r_{Pt-Pt}, at $\mathbf{k} = 0$.

The reader will notice that the s and $d_{x^2-y^2}$ bands are missing from Figure 1. They are of course present, but at much higher energy. The $x^2 - y^2$ level is destabilized by interactions with the cyanides within a monomer, and the s band is pushed up by intermonomer mixing with d_{z^2}.

B. Band Structure as a Function of r_{Pt-Pt}. Figure 2 shows the top and bottom portions, respectively, of the filled and empty bands of the $Pt(CN)_4^{2-}$ chain as a function of r_{Pt-Pt}. For the purpose of simplicity, only the d_{z^2} and p_z [mixed with $\pi^*(CN)$] bands are shown. As r_{Pt-Pt} decreases, the widths of these two bands expand leading to a small band gap between the two.[4c] When r_{Pt-Pt} reaches a certain point (approximately 2.7 Å), a further decrease in r_{Pt-Pt} results in a wider band gap. In this region the top of the d_{z^2} band shows p_z orbital character for Pt, while the bottom of the p_z band has d_{z^2} orbital character for Pt. As plotted in Figure 3, there occurs a smooth change in the orbital characters of the top of the d_{z^2} band and the bottom of the p_z band. The rationale for this will be explored in the next section. It may be inferred from Figure 3 that the d_{z^2} and p_z bands would not overlap as in semimetals when r_{Pt-Pt} varies.

C. Qualitative Description of Band Formation. The structures of the d_{z^2} and p_z bands of Figure 2 may now be described qualitatively. For the sake of simplicity, let us consider only the two Pt atoms in a unit cell and their d_{z^2} orbitals. In a unit cell these two d_{z^2} orbitals lead to in-phase, $d_{z^2}^+$, and out-of-phase, $d_{z^2}^-$, combinations. The most stable state is obtained by combining the $d_{z^2}^+$ orbitals in-phase between neighboring unit

$d_{z^2}^+$ $\qquad$ $d_{z^2}^-$

cells, **4**. This corresponds to the bottom of the d_{z^2} band, $\mathbf{k} = 0$. The most unstable state results from the out-of-phase combination of the $d_{z^2}^-$ orbitals, **5**, leading to the top of the d_{z^2} band.

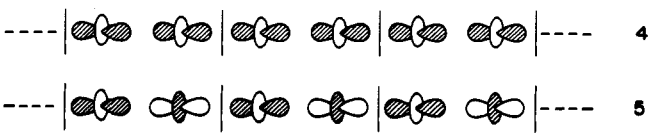

The least stable combination of the $d_{z^2}^+$ orbitals, **6**, and the most stable combination of the $d_{z^2}^-$ orbitals, **7**, are the same in energy, given the translational symmetry. This accounts for the degeneracy of the d_{z^2} band at the zone boundary.

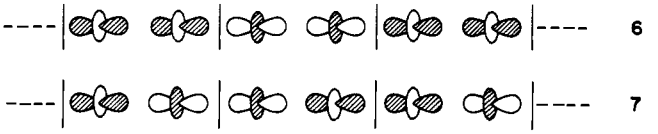

By considering the in-phase, p_z^+, and out-of-phase, p_z^-, combinations of the two platinum p_z orbitals, the structure of

p_z^+ $\qquad$ p_z^-

the p_z band may be described in a manner similar to the above. With the decrease of r_{Pt-Pt} the splitting between $d_{z^2}^+$ and $d_{z^2}^-$ (and that between p_z^+ and p_z^- as well) becomes large, so that the p_z^+ level eventually lies lower than the $d_{z^2}^-$ level (**8**).

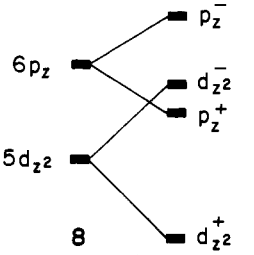

Therefore, according to the above discussion, it might be expected that the resulting p_z and d_{z^2} bands should overlap appreciably. This would happen if the overlap between the p_z^+ and p_z^- orbitals of a unit cell and the $d_{z^2}^+$ and $d_{z^2}^-$ orbitals of its neighbor unit cells is negligible. However, the shortening of r_{Pt-Pt} not only provides the large splitting of the levels, but it also enhances the magnitude of the aforementioned overlap. An avoided crossing situation arises, with separation of the bands but an actual interchange of p and d character as if the crossing had in fact taken place.

In Figure 2 it was observed that as r_{Pt-Pt} decreased the two bands came closer together at $\mathbf{k} = 0$ and then diverged. Figure 3 showed that an actual crossing occurs. As is shown in **9** and **10**, the $d_{z^2}^-$ level at the zone center ($\mathbf{k} = 0$) is symmetric with

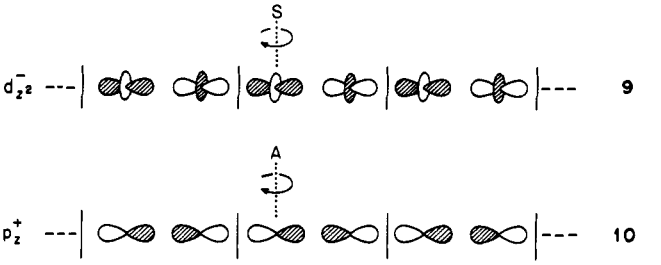

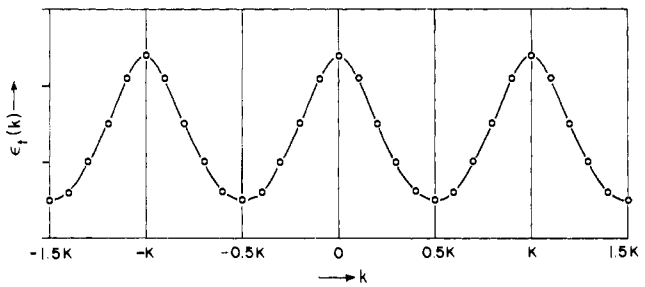

Figure 4. Plot of $\epsilon_t(\mathbf{k})$ against $\mathbf{k}$ for $r_{Pt-Pt} = 2.88$ Å. The cubic spline fitting was carried out for the region $-1.5K \leq \mathbf{k} \leq 1.5K$.

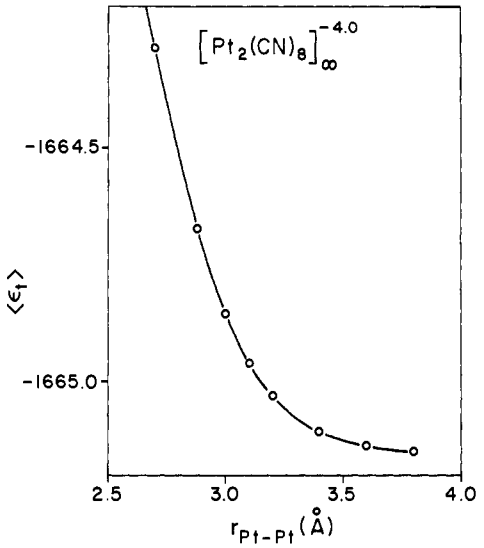

Figure 5. The total energy per unit cell for the unoxidized $Pt(CN)_4^{2-}$ chain as a function of r_{Pt-Pt}.

respect to a symmetry operation, while the p_z^+ is antisymmetric. Only at this point in $\mathbf{k}$ space the levels may cross.

Partial Oxidation and Free Electron Behavior of the d_{z^2} Band Electrons

When there is no oxidation of the $Pt(CN)_4^{2-}$ chain, the d_{z^2} band is fully occupied. The top portion of this band is largely antibonding in character between the Pt atoms. Electron removal from the d_{z^2} band by partial oxidation will decrease this antibonding nature, so that the bonding between the Pt atoms is strengthened. The concomitant shortening of r_{Pt-Pt} follows. In this section this point will be examined by evaluating the total energy per unit cell,[6c,9b] $\langle\epsilon_t\rangle$, for the $Pt(CN)_4^{2-}$ chain as a function of r_{Pt-Pt}.

In the absence of oxidation, $\langle\epsilon_t\rangle$ of the $Pt(CN)_4^{2-}$ chain is given by

$$\langle\epsilon_t\rangle = \frac{1}{K}\int_{-K/2}^{K/2} \epsilon_t(\mathbf{k})d\mathbf{k} \tag{4}$$

where $\epsilon_t(\mathbf{k})$ is the total energy at $\mathbf{k}$,

$$\epsilon_t(\mathbf{k}) = 2\sum_{n}^{occ} \epsilon_n(\mathbf{k}) \tag{5}$$

The simple summation of one-electron eigenvalues is a typical feature of extended Hückel calculations. It appears that the Coulombic repulsions, both intra- and intercell, are in some way included in the extended Hückel energies. Though there have been several attempts to derive this formalism, perhaps the best justification for its use is to be found in its success in describing a wide range of organic and inorganic geometrical problems.

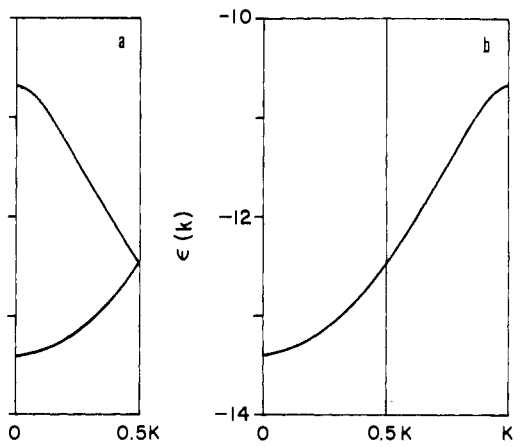

Figure 6. The structure of the d_{z^2} band for $r_{Pt-Pt} = 2.88$ Å; (a) folded structure and (b) unfolded structure. The cubic spline fitting was carried out after repeating the unfolded structure as in Figure 4 for the region $-3K \leq \mathbf{k} \leq 3K$.

The $\epsilon_t(\mathbf{k})$ values are available only for the $\mathbf{k}$ points at which eq 2 is actually solved. By applying the cubic spline curve fitting procedure (with the boundary condition that $\partial^2\epsilon_t(\mathbf{k})/\partial\mathbf{k}^2 = 0$)[11] to these values, an analytical expression for $\epsilon_t(\mathbf{k})$ was obtained. In order that the resulting splines become continuous at the zone center and boundaries,[12] the curve fitting was carried out for the extended zone as shown in Figure 4. In the evaluation of eq 4 only the splines of the middle region (i.e., $-0.5K \leq \mathbf{k} \leq 0.5K$) were used.

The results of the above calculations are summarized in Figure 5, which shows no indication that the $Pt(CN)_4^{2-}$ chain is bound. At $r_{Pt-Pt} = 3.8$ Å the chain is less stable than the isolated $Pt(CN)_4^{2-}$ complex by about 2 kcal/mol per unit cell. The neutron diffraction study[2n] of $K_2Pt(CN)_4{\cdot}3H_2O$ reveals that r_{Pt-Pt} is about 3.48 Å, and alternate $Pt(CN)_4^{2-}$ units are nearly eclipsed. At $r_{Pt-Pt} = 3.48$ Å the present calculation has the $Pt(CN)_4^{2-}$ chain unstable with respect to the isolated $Pt(CN)_4^{2-}$ complex about 3 kcal/mol per unit cell. The observed stability of $K_2Pt(CN)_4{\cdot}3H_2O$ probably results in large part from the hydrogen bonding by the water molecules, which link the CN^- ligands within a $Pt(CN)_4^{2-}$ stack, as well as cross-link adjacent $Pt(CN)_4^{2-}$ stacks.[2n] Also extended Hückel calculations do not include the attractive part of the van der Waals potential.

When the $Pt(CN)_4^{2-}$ chain is partially oxidized, the evaluation of $\langle\epsilon_t\rangle$ becomes more complicated than described above. In the following we first examine the nature of the d_{z^2} band, from which electrons are removed by partial oxidation.

A. Free Electron Nature of the d_{z^2} Band Electrons. To calculate $\langle\epsilon_t\rangle$ for the partially oxidized states, one has to determine the Fermi level ϵ_f or the Fermi momentum $\mathbf{k}_f$. This requires knowledge of the integrated density of states,[13] $n(\epsilon)$, for the d_{z^2} band. Here $n(\epsilon)$ means the number of electrons per unit cell when the levels are occupied up to ϵ. The expression for $n(\epsilon)$ is

$$n(\epsilon) = \int_{\epsilon_b}^{\epsilon} g(\epsilon)d\epsilon \tag{6}$$

where ϵ_b is the bottom of the d_{z^2} band, and the density of state, $g(\epsilon)$, is given by

$$g(\epsilon) = \frac{1}{\pi}\frac{d\mathbf{k}}{d\epsilon(\mathbf{k})} \tag{7}$$

for one-dimensional systems.

An analytical expression for $\epsilon(\mathbf{k})$ for the d_{z^2} band was determined by unfolding the upper part of the band of the first zone onto the second zone (Figure 6) and by applying the cubic

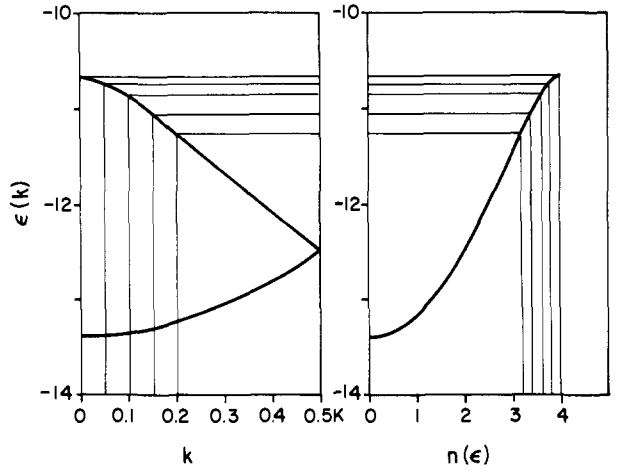

Figure 7. The d_{z^2} band and its integrated density of states for $r_{Pt-Pt} = 2.88$ Å. The lines show the correlation between δ and $\mathbf{k}_f$.

Table I. Effective Masses[a] at the Top (m_t*) and Bottom (m_b*) and the Gaps at Various Pt-Pt Separations

r_{Pt-Pt}, Å	Δ_g, eV	m_b*	m_t*
2.88	0.68	1.00	−0.14
3.0	1.11	1.14	−0.26
3.1	1.42	1.29	−0.39
3.2	1.68	1.48	−0.54
3.4	2.08	1.96	−1.02

[a] The effective masses are given in units of m_e, the free electron mass.

spline fitting procedure to the unfolded band. With the splines thus obtained $n(\epsilon)$ was calculated by numerical integration. In the small regions of $\mathbf{k} = -K, 0, K$ where the slope of $\epsilon(\mathbf{k})$ vanishes, $\epsilon(\mathbf{k})$ was assumed to be parabolic, so that the integration of eq 6 can be performed analytically.

The results of this analysis are shown in Figure 7 for $r_{Pt-Pt} = 2.88$ Å, where $n(\epsilon)$ is normalized such that $n(\epsilon)$ becomes four electrons at the top of the d_{z^2} band. Since a true unit cell contains *two* $Pt(CN)_4^{2-}$ subunits, the partial oxidation state of $Pt^{2+\delta}$ corresponds to electron removal of 2δ per unit cell. From examination of $n(\epsilon)$ it is observed that, for $\delta = 0.1, 0.2, 0.3, 0.4$, and 0.5, the Fermi momenta $\mathbf{k}_f$ turn out nearly 0.05, 0.10, 0.15, 0.20, and $0.25K$ (in the extended zone of Figure 6b they are 0.95, 0.90, 0.85, 0.80, and $0.75K$), respectively.[14] This property of $n(\epsilon)$ is what one expects from free electrons. The analysis of $n(\epsilon)$ at other values of r_{Pt-Pt} reveals almost the same correlation between $\mathbf{k}_f$ and δ as the above. These results are in agreement with experiment.[3]

From the analytical expression for $\epsilon(\mathbf{k})$ already determined, the effective mass m* of electrons was calculated at the bottom (m_b*) and at the top (m_t*) of the d_{z^2} band. Table I lists these values of m* at various values of r_{Pt-Pt} along with the band gap Δ_g between the d_{z^2} and p_z bands. The top of the d_{z^2} band is the region which differs most from the free electron band, so that the m_t* values show a large departure from m_e. The narrow bandwidths at a large r_{Pt-Pt} is reflected in the large magnitude of m*.

B. Partial Oxidation and r_{Pt-Pt}. The d_{z^2} band overlaps with other bands as was seen in Figure 1. However, according to our band structures, it is found that, up to the partial oxidation of $\delta \simeq 0.8$, electron removal occurs from the d_{z^2} band. With the Fermi momentum $\mathbf{k}_f$ and the analytical expression of $\epsilon(\mathbf{k})$ it is straightforward to calculate the energy loss per unit cell caused by electron removal and thus to calculate $\langle \epsilon_t \rangle$ for partially oxidized states. The results of this study are shown

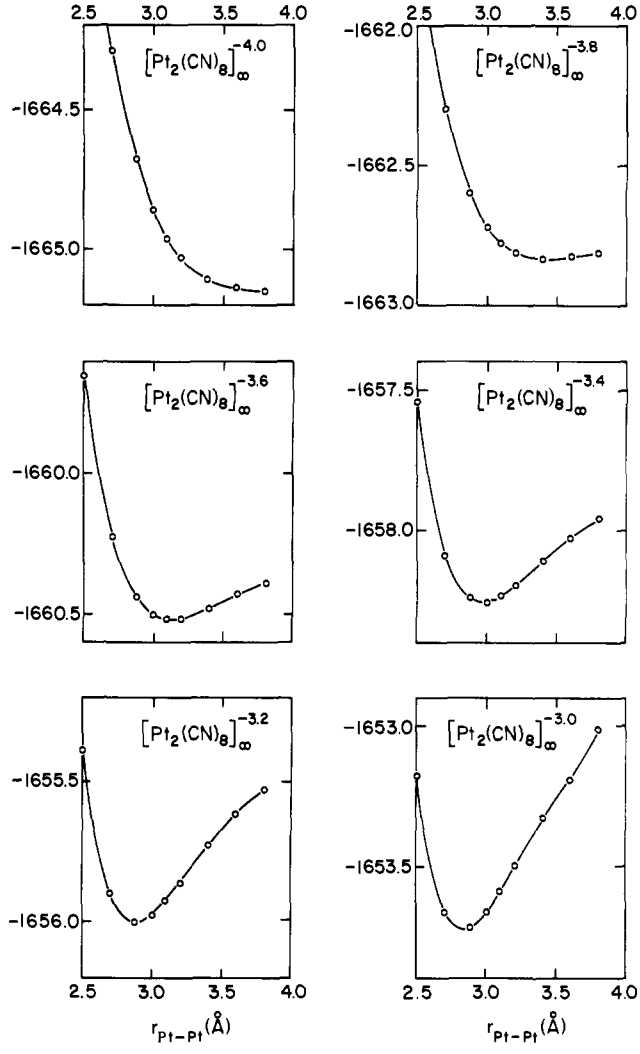

Figure 8. The total energy per unit cell for the partially oxidized $Pt(CN)_4^{2-}$ chain as a function of r_{Pt-Pt}. The six graphs show δ increasing from 0 to 0.5.

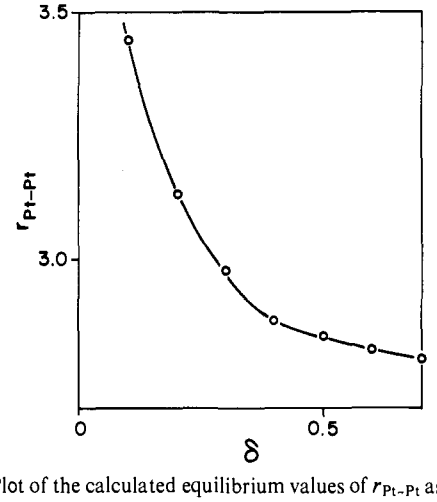

Figure 9. Plot of the calculated equilibrium values of r_{Pt-Pt} as a function of δ.

in Figure 8 for $\delta = 0.1, 0.2, 0.3, 0.4$, and 0.5. All these partially oxidized states are found to be bound, and the equilibrium value of r_{Pt-Pt} decreases with increasing partial oxidation number. The estimated equilibrium values of r_{Pt-Pt} are 3.44, 3.13, 2.99, 2.88, and 2.85 Å for $\delta = 0.1, 0.2, 0.3, 0.4$, and 0.5, respectively. Figure 9 shows the calculated equilibrium values

Table II. Atomic Parameters

χ_μ	ζ_μ	$H_{\mu\mu}$
C 2s	1.625	−21.4
C 2p	1.625	−11.4
N 2s	1.950	−26.0
N 2p	1.950	−13.4
Pt 5d	*a*	−12.6
Pt 6s	2.554	−9.08
Pt 6p	2.554	−5.48

[a] A linear combination of the two Slater orbitals of exponents 6.013 and 2.696 with weighting coefficients 0.6334 and 0.5513, respectively (ref 18).

of r_{Pt-Pt} as a function of δ. It is found that the differential shortening of r_{Pt-Pt} becomes smaller as δ increases. This trend is in good agreement with experiment[1,2] and also with the empirical correlation[15] obtained from Pauling's bond distance–bond number relationship.[16]

The occurrence of minima in the potential energy curves of the oxidized states may be understood by reference to Figure 2. At a large value of r_{Pt-Pt} the d_{z^2} bandwidth is small owing to small overlap between neighbor cells. Therefore at larger r_{Pt-Pt} the top portion of the d_{z^2} band has less antibonding character, in turn leading to greater energy loss upon partial oxidation.

These calculations give a description of the band structure of the tetracyanoplatinate chain that is in reasonable agreement with other calculations and the experimental facts. The extended Hückel procedure generally does not do well at bond distance variation, so it was both surprising and encouraging that it gives reasonable Pt-Pt separations as a function of the degree of oxidation. In future papers we will use the methodology developed here to probe conformational preferences in other known one- and two-dimensional cases, and attempt to design some novel conducting systems.

Acknowledgment. We are grateful to the National Science Foundation for its support of this work through Grant CHE-76-06099, and to E. Kronman for the typing and J. Jorgensen for the drawings.

Appendix

Atomic parameters of the extended Hückel method (i.e., exponents ζ_μ and valence state ionization potentials $H_{\mu\mu}$ for atomic basis orbitals χ_μ) employed in the present work are listed in Table II. Off-diagonal matrix elements $H_{\mu\nu}$ of the effective Hamiltonian were calculated according to the modified Wolfsberg-Helmholz formula.[17]

References and Notes

(1) For reviews see J. S. Miller and A. J. Epstein, *Prog. Inorg. Chem.*, **20**, 1 (1976); K. Krogmann, *Angew. Chem.*, **81**, 10 (1969); *Angew. Chem., Int. Ed. Engl.*, **8**, 35 (1969).
(2) (a) R. M. Bozorth and L. Pauling, *Phys. Rev.*, **39**, 537 (1932); (b) H. Brasseur and A. deRassenfosse, *Mem. Soc. R. Sci. Liège*, **18**, 1 (1933); (c) H. Lambot, *Bull. Soc. R. Sci. Liège*, **12**, 522 (1943); (d) F. Fontaine, *ibid.*, **33**, 178 (1964); (e) K. Krogmann and H. D. Hausen, *Z. Anorg. Allg. Chem.*, **358**, 67 (1968); (f) J. M. Williams, J. L. Petersen, H. M. Gerdes, and S. W. Peterson, *Phys. Rev. Lett.*, **33**, 1079 (1974); (g) J. M. Williams, M. Iwata, S. W. Peterson, K. A. Leslie, and H. J. Guggenheim, *ibid.*, **34**, 1653 (1975); (h) C. Peters and C. F. Eagan, *ibid.*, **34**, 1132 (1975); (i) J. M. Williams, F. K. Ross, M. Iwata, J. L. Petersen, S. W. Peterson, S. C. Lin, and K. D. Keefer, *Solid State Commun.*, **17**, 45 (1975); (j) J. M. Williams, M. Iwata, F. K. Ross, J. L. Petersen, and S. W. Peterson, *Mater. Res. Bull.*, **10**, 411 (1975); (k) G. Heger, B. Renker, H. Deiseroth, H. Schulz, and G. Scheiber, *ibid.*, **10**, 217 (1975); (l) K. D. Keefer, D. M. Washecheck, N. P. Enright, and J. M. Williams, *J. Am. Chem. Soc.*, **98**, 233 (1976); (m) A. H. Reis, Jr., S. W. Peterson, D. M. Washecheck, and J. S. Miller, *ibid.*, **98**, 234 (1976); *Inorg. Chem.*, **15**, 2455 (1976); (n) D. M. Washecheck, S. W. Peterson, A. H. Reis, Jr., and J. M. Williams, *ibid.*, **15**, 74 (1976); (o) J. M. Williams, K. D. Keefer, D. M. Washecheck, and N. P. Enright, *ibid.*, **15**, 2446 (1976); (p) P. L. Johnson, T. R. Koch, and J. M. Williams, *Acta Crystallogr., Sect. B*, **33**, 1293 (1977).
(3) (a) D. Kuse and H. R. Zeller, *Phys. Rev. Lett.*, **27**, 1060 (1971); *Solid State Commun.*, **11**, 355 (1972); (b) H. P. Geserich, H. D. Hausen, K. Krogmann, and P. Stampfl, *Phys. Status Solidi A*, **9**, 187 (1972); (c) H. Wagner, H. P. Geserich, R. v. Baltz, and K. Krogmann, *Solid State Commun.*, **13**, 659 (1973); (d) R. Comès, M. Lambert, H. Launois, and H. R. Zeller, *Phys. Rev. Sect. B*, **8**, 571 (1973); (e) B. Renker, H. Rietschel, L. Pintschovius, W. Gläser, P. Brüesch, D. Kuse, and M. J. Rice, *Phys. Rev. Lett.*, **30**, 1144 (1973); (f) H. R. Zeller and P. Brüesch, *Phys. Status Solidi B*, **65**, 537 (1974); (g) J. Bernasconi, P. Brüesch, D. Kuse, and H. R. Zeller, *J. Phys. Chem. Solids*, **35**, 145 (1974).
(4) (a) R. P. Messmer and D. R. Salahub, *Phys. Rev. Lett.*, **35**, 533 (1975); (b) D. M. Whitmore, Ph.D. Thesis, Stanford University, 1974; (c) H. Yersin, G. Gliemann and U. Rössler, *Solid State Commun.*, **21**, 915 (1977).
(5) (a) For some related calculations see L. V. Interrante and R. P. Messmer, *Inorg. Chem.*, **10**, 1174 (1971); ACS Symposium Series No. 5, "Extended Interactions between Metal Ions in Transition Metal Complexes," American Chemical Society, Washington, D.C., 1974, p 382; (b) D. W. Bullett, to be published.
(6) (a) J.-M. André, *J. Chem. Phys.*, **50**, 1536 (1969); (b) J.-M. André, "Electronic Structure of Polymers and Molecular Crystals", J.-M. André and J. Ladik, Ed., Plenum Press, New York, N.Y., 1974, p 1; (c) J. Ladik, *ibid.*, p 23.
(7) R. Hoffmann, *J. Chem. Phys.*, **39**, 1397 (1963); R. Hoffmann and W. N. Lipscomb, *ibid.*, **36**, 2179, 3489 (1962); **37**, 2872 (1962).
(8) For some readable introductions to solid-state theory see (a) M. H. B. Stiddard, "The Elementary Language of Solid State Physics", Academic Press, New York, N.Y., 1975; (b) S. L. Altmann, "Band Theory of Metals", Pergamon Press, Oxford, 1970; (c) N. W. Ashcroft and N. D. Mermin, "Solid State Physics", Holt, Rinehart and Winston, New York, N.Y., 1976.
(9) The following are the earlier of many possible references: (a) W. L. McCubbin and R. Manne, *Chem. Phys. Lett.*, **2**, 230 (1968); (b) A. Imamura, *J. Chem. Phys.*, **52**, 3168 (1970); (c) R. P. Messmer, *Chem. Phys. Lett.*, **11**, 589 (1971).
(10) This has also been observed by R. P. Messmer and L. V. Interrante in their band structure calculations (cited in ref 3f).
(11) (a) E. N. Nilson, *Commun. ACM*, **13**, 255 (1970); (b) T. N. E. Grenville, "Mathematical Methods for Digital Computers", Vol. 2, Wiley, New York, N.Y., 1967, Chapter 8.
(12) M. Lax, "Symmetry Principles in Solid State and Molecular Physics", Wiley, New York, N.Y., 1974, Chapter 7.
(13) (a) J. Delhalle, "Electronic Structure of Polymers and Molecular Crystals", J.-M. Andrè and J. Ladik, Ed., Plenum Press, New York, N.Y., 1974, p 53; (b) J. Delhalle and S. Delhalle, *Int. J. Quantum Chem.*, **11**, 349 (1977).
(14) For instance, at r_{Pt-Pt} = 2.88 Å, k_l = 0.0485, 0.0986, 0.1487, 0.1989, and 0.2491*K* for δ = 0.1, 0.2, 0.3, 0.4, and 0.5, respectively.
(15) A. H. Reis, Jr., and S. W. Peterson, *Inorg. Chem.*, **15**, 3186 (1976).
(16) (a) L. Pauling, *J. Am. Chem. Soc.*, **69**, 542 (1947); (b) *Nature (London)*, **161**, 1019 (1948).
(17) (a) R. Hoffmann and P. Hofmann, *J. Am. Chem. Soc.*, **98**, 598 (1976); (b) J. H. Ammeter, H.-B. Bürgi, J. C. Thibeault, and R. Hoffmann, *ibid.*, **100**, 3686 (1978).
(18) R. H. Summerville and R. Hoffmann, *J. Am. Chem. Soc.*, **98**, 7240 (1976).